

Debye–Waller parameters of diatomic crystals

M. INAGAKI, M. TOYODA, M. SAKAI

Materials Science, Toyohashi University of Technology, Tempaku-cho, Toyohashi, 440 Japan

The Debye–Waller parameters, the effective values B_{eff} , the dynamic component, B_{d} , and the static component, B_{s} , of each constituent atom and also of the bulk were measured for some diatomic crystals with NaCl- and zinc blende-type structures. The dominant effect of heavy constituent atoms on the dynamic component of bulk crystals was found, and the mean square displacement in bulk crystals was approximated well by the atomic mass averaged mean square displacements of the constituent atoms. A remarkable effect of structural defects on B_{eff} , particularly on B_{s} , was observed in NiO samples with different degrees of non-stoichiometry. The different extents of the SiC-forming reaction between solid carbon and fused silicon resulted in quite different B_{eff} values; the larger the B_{eff} value the smaller the extent of the reaction.

1. Introduction

In previous papers [1, 2], monoatomic crystals, isotropic palladium metal and anisotropic graphite, were studied in order to discuss the Debye–Waller parameters. The effective Debye–Waller parameter, B_{eff} , which was determined from the plots of integrated intensity of X-ray diffraction lines against $\sin^2\theta/\lambda^2$, was understood to consist of two components, i.e. dynamic and static, B_{d} and B_{s} , the former being due to thermal vibration of constituent atoms and the latter to the static displacement of atoms from the equilibrium lattice points. These two components were evaluated separately from the temperature dependence of B_{eff} under the assumptions of a linear combination of B_{d} and B_{s} , and of no annealing of lattice defects below room temperature. In the case of anisotropic crystal structure, as in graphite, these Debye–Waller parameters had to be determined along each crystal axis. The Debye temperatures, θ_{D} , calculated from B_{d} of the substances, were closely related to its B_{s} value. For palladium metal powders, the presence of a static component was qualitatively explained by the distorted surface layers on each particle (core–shell model) [1]. For carbon materials, θ_{D} and B_{s} were discussed in relation to conventional structural parameters, such as interlayer spacing, etc. [2].

The same discussions can be held for crystals comprising different atoms. If diatomic crystals with NaCl- or zinc blende-type structure are chosen as samples, the Debye–Waller parameters for each constituent atom can be determined separately from the series of diffraction lines with different combinations of Miller indices. It would clearly be advantageous if X-ray diffraction analysis was able to determine the Debye temperature for each constituent atom as well as for the bulk crystal.

In the present work, the effective Debye–Waller parameter, B_{eff} , of the constituent atoms in some diatomic crystals with either NaCl- or zinc blende-type structures were determined and separated into dynamic and static components using their tempera-

ture dependencies. The relationship of the B -values of bulk crystals to those of constituent atoms is discussed.

2. Theoretical determinations

2.1. Determination of B values of the constituent atoms

In sodium chloride-type AX crystals, the B_{eff} value of each atom, $B_{\text{eff}}(\text{A})$ and $B_{\text{eff}}(\text{X})$, can be determined by the following procedure, as shown by Warren [3] for NaCl. Q is calculated from the observed intensity, I_{obs} :

$$Q = I_{\text{obs}}/pALP, \quad (1)$$

is proportional to the structure amplitude of the hkl line and is expressed as follows:

when all indices are even,

$$Q(\text{even}) = K \{ f_{\text{A}} \exp[-B_{\text{eff}}(\text{A}) \sin^2\theta/\lambda^2] + f_{\text{X}} \exp[-B_{\text{eff}}(\text{X}) \sin^2\theta/\lambda^2] \} \quad (2a)$$

and when all indices are odd,

$$Q(\text{odd}) = K \{ f_{\text{A}} \exp[-B_{\text{eff}}(\text{A}) \sin^2\theta/\lambda^2] - f_{\text{X}} \exp[-B_{\text{eff}}(\text{X}) \sin^2\theta/\lambda^2] \} \quad (2b)$$

In the above equations, p is a multiplicity of the hkl lines, A is the absorption factor, LP is the Lorentz-polarization factor, K is a proportional constant, f_{A} and f_{X} are atomic scattering factors for A and X, respectively. From Equations 2a and b,

$$\begin{aligned} \ln \{ [Q(\text{even}) + Q(\text{odd})]/2f_{\text{A}} \} \\ = \ln K - B_{\text{eff}}(\text{A}) \sin^2\theta/\lambda^2 \end{aligned} \quad (3a)$$

$$\begin{aligned} \ln \{ [Q(\text{even}) - Q(\text{odd})]/2f_{\text{X}} \} \\ = \ln K - B_{\text{eff}}(\text{X}) \sin^2\theta/\lambda^2 \end{aligned} \quad (3b)$$

are obtained. These equations indicate that $B_{\text{eff}}(\text{A})$ and $B_{\text{eff}}(\text{X})$ are given as the slopes of the plots of $\ln \{ [Q(\text{even}) \pm Q(\text{odd})]/2f \}$ against $\sin^2\theta/\lambda^2$.

Similar to NaCl-type crystals, the Q -values of zinc blende-type AX crystal are expressed as follows:

when the indices are all even and their sum equals $4n$,

$$Q(\text{even}) = K \{ f_X \exp [-B_{\text{eff}}(\text{X}) \sin^2 \theta / \lambda^2] + f_A \exp [-B_{\text{eff}}(\text{A}) \sin^2 \theta / \lambda^2] \} \quad (4a)$$

when the indices are all even but their sum equals $2(2n + 1)$,

$$Q'(\text{even}) = K \{ f_X \exp [-B_{\text{eff}}(\text{X}) \sin^2 \theta / \lambda^2] - f_A \exp [-B_{\text{eff}}(\text{A}) \sin^2 \theta / \lambda^2] \} \quad (4b)$$

and when the indices of the diffraction line are all odd,

$$Q(\text{odd}) = K \{ f_A \exp [-2B_{\text{eff}}(\text{A}) \sin^2 \theta / \lambda^2] + f_X \exp [-2B_{\text{eff}}(\text{X}) \sin^2 \theta / \lambda^2] \} \quad (4c)$$

then, the following equations are deduced from Equations 4a and b:

$$\begin{aligned} \ln \{ [Q(\text{even}) + Q'(\text{even})] / 2f_X \} \\ = \ln K - B_{\text{eff}}(\text{X}) \sin^2 \theta / \lambda^2 \end{aligned} \quad (5a)$$

$$\begin{aligned} \ln \{ [Q(\text{even}) - Q'(\text{even})] / 2f_A \} \\ = \ln K - B_{\text{eff}}(\text{A}) \sin^2 \theta / \lambda^2 \end{aligned} \quad (5b)$$

As in the case of NaCl-type crystals, the effective Debye–Waller parameters for each atom are determined as the slopes of $\ln \{ [Q(\text{even}) \pm Q'(\text{even})] / 2f \}$ plotted against $\sin^2 \theta / \lambda^2$.

2.2. Determination of B values of the bulk crystals

The effective Debye–Waller parameter of a bulk crystal AX, $B_{\text{eff}}(\text{AX})$, is determined from the plots of $\ln [I_{\text{obs}}(hkl) / I_{\text{calc}}(hkl)]$ against $\sin^2 \theta / \lambda^2$ using the following equation

$$\begin{aligned} \ln [I_{\text{obs}}(hkl) / I_{\text{calc}}(hkl)] \\ = \ln K - 2B_{\text{eff}}(\text{AX}) \sin^2 \theta / \lambda^2 \end{aligned} \quad (6)$$

For NaCl-type crystals, two parallel relations are obtained, one for diffraction lines with even indices and the other for those with odd indices. For zinc blende-type crystals, three parallel relations exist for three different combinations of indices.

2.3. Separation of B_{eff} values into dynamic and static components

All of the empirical Debye–Waller parameters for each atom and the bulk crystal are the effective values and are related to the dynamic and static components, B_d and B_s [1]

$$B_{\text{eff}} = B_d + B_s \quad (7)$$

The temperature dependence of B_d is given by the Debye equation

$$\begin{aligned} B_d &= (6h^2 T / mk \theta_D) [\phi(x) + (x/4)] \\ \phi(x) &= \frac{1}{x} \int_0^x \frac{\varepsilon}{\varepsilon - 1} d\varepsilon, \quad x = \theta_D / T \end{aligned} \quad (8)$$

and B_s is approximated to be independent of ambient temperature below room temperature, which means that two components B_d and B_s are calculated from two B_{eff} values for two different temperatures. In Equation 8, h is Planck's constant, m is the mass, and k is the Boltzmann constant. The detailed procedure for this separation has been reported before [1].

3. Experimental details and results

The samples with either NaCl- or zinc blende-type crystal structure used in the present work are listed in Table I with a short description of their preparations.

Nine to eleven diffraction lines, each of which did not overlap with neighbouring lines, were chosen in a $\sin^2 \theta / \lambda^2$ range of 0.0002 to 0.0031 nm². The integrated intensity of each line was determined by summing the diffraction intensities measured in every 0.02° or 0.05° step in 2θ by fixed time (40 sec) method and subtracting the background intensity. The nickel-filtered $\text{CuK}\alpha$ radiation and scintillation counter with pulse height analyzer were employed. Diffraction intensity measurements were carried out in vacuum at room temperature and 80 K.

From the experimental $I_{\text{obs}}(hkl)$ and $I_{\text{calc}}(hkl)$ -derived Q values (Equation 1) for each line, effective values of Debye–Waller parameters, B_{eff} , were determined through the procedure explained in the previous section. The atomic scattering factors for each

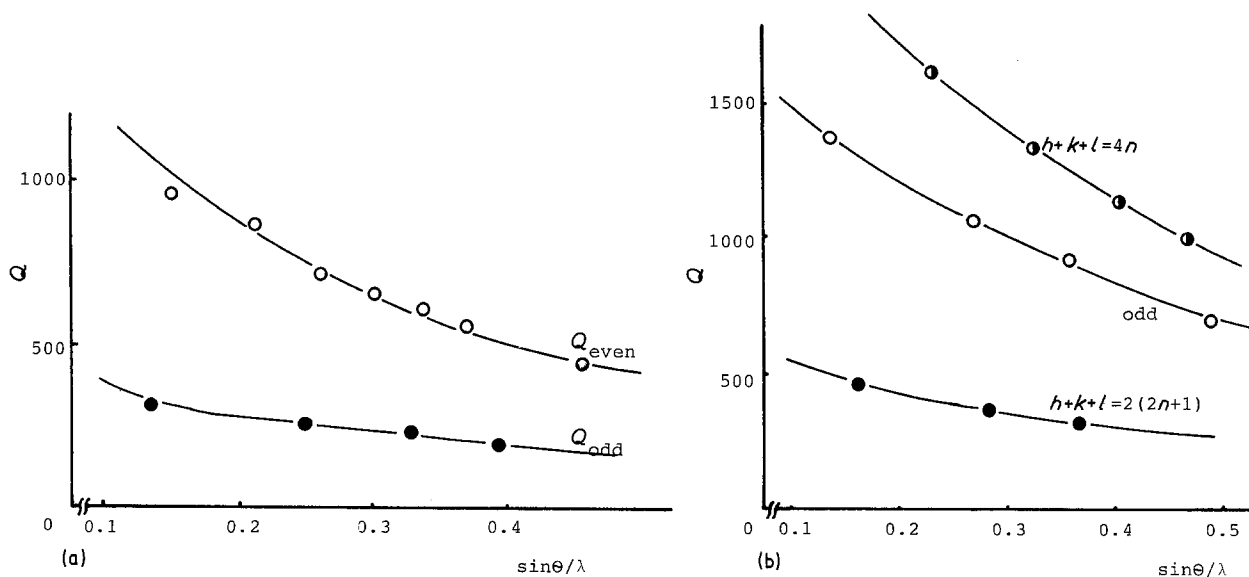


Figure 1 Relations between Q and $\sin \theta / \lambda$. (a) KBr (NaCl-type), (b) ZnTe (zinc blende-type).

TABLE I Dynamic component, B_d , and static component, B_s , in Debye–Waller parameters and Debye temperature, θ_D , of diatomic crystals

Sample	Raw material, preparation	Bulk			Cation			Anion		
		θ_D (K)	B_d (10^{-2} nm^2)	B_s (10^{-2} nm^2)	θ_D (K)	B_d (10^{-2} nm^2)	B_s (10^{-2} nm^2)	θ_D (K)	B_d (10^{-2} nm^2)	B_s (10^{-2} nm^2)
<i>NaCl-type structure</i>										
CdO	Reagent grade	352	0.42	0.27	267	0.42	0.45	879	0.41	0.75
NiO	NiNO ₃ , 1000°C, argon	480	0.22	0.44	540	0.22	0.53	840	0.37	0.57
	1000°C, air	480	0.22	0.86	500	0.23	1.04	690	0.52	1.00
MgO	Mg(OH) ₂ , 850°C,	450	0.45	0.19	550	0.50	0.40	940	0.41	0.41
KBr	Reagent grade, 110°C, <i>in vacuo</i>	240	0.49	0.98	670	0.22	1.28	310	0.46	1.02
PbS		173	0.96	0.27	123	1.09	0.22	455	0.60	0.0
<i>Zinc blende-type structure</i>										
SiC	Pulverizing whisker	540	0.32	0.32	660	0.31	0.17	1000	0.38	0.94
	reaction of C with Si:									
	48% SiC	530	0.32	0.43	570	0.40	0.22			
	26% SiC	310	0.89	0.74	400	0.79	0.63			
BN	c-BN, 325/400 mesh	520	0.53	0.73				880	0.38	1.71
GaP	Pulverizing single crystal	232	0.62	0.78	290	0.59	1.71	340	0.99	1.77
ZnTe	As-received	210	0.40	0.48	330	0.49	0.53	290	0.32	0.61
	3.5 h ground	230	0.32	1.58	250	0.83	2.98	160	1.07	1.72
	6.5 h ground	230	0.34	2.10	200	1.28	3.36	180	0.84	2.32

atom were obtained from the published data [4], and the absorption factor A was calculated from the mass absorption factor for each atom and the bulk density of the sample powder in the X-ray sample holder.

In Fig. 1a, the plots of Q against $\sin \theta/\lambda$ for KBr (NaCl-type crystal) are shown, as an example. For NaCl-type crystals, four pairs of diffraction lines with all even and odd indices were chosen. The slopes of the linear relations between $\ln \{[Q(\text{even}) \pm Q(\text{odd})]/2f\}$ and $\sin^2 \theta/\lambda^2$ yielded $B_{\text{eff}}(\text{A})$ and $B_{\text{eff}}(\text{X})$ values according to Equations 3a and b. Usually the experimental points of $\ln \{[Q(\text{even}) + Q(\text{odd})]/2f\}$ for heavy atoms indicated less scattering than with those of $\ln \{[Q(\text{even}) - Q(\text{odd})]/2f\}$ for light atoms. Therefore, the relation for the heavy atoms was first determined and then the line for the light atoms was determined in order to give the same intercept ($\ln K$) at $\sin^2 \theta/\lambda^2 = 0$. The details of experimental analysis have been discussed using PbS [5].

With zinc blende-type crystals, three pairs of diffraction lines with even indices were chosen such that their sums were $4n$ and $2(2n + 1)$, n being an integer. Using a similar procedure in NaCl-type crystals, and Equations 5a and b, the values of $B_{\text{eff}}(\text{A})$ and $B_{\text{eff}}(\text{X})$ were determined. The plots of Q against $\sin \theta/\lambda$ for ZnTe are shown as an example in Fig. 1b.

The $B_{\text{eff}}(\text{AX})$ -values for bulk crystals were determined from the slopes of $\ln [I_{\text{obs}}/I_{\text{calc}}]$ against $\sin^2 \theta/\lambda^2$ relation through Equation 6: there are two linear relations for the diffraction lines with all even and with all odd indices for NaCl-type crystals, and three parallel relations for three distinct combinations of indices of zinc blende-type crystals.

Accuracy in the B_{eff} values was $\pm 0.0002 \text{ nm}^2$ for heavy atoms, $\pm 0.0004 \text{ nm}^2$ for light atoms and $\pm 0.0002 \text{ nm}^2$ for bulk crystals.

From the values of $B_{\text{eff}}(\text{A})$, $B_{\text{eff}}(\text{X})$ and $B_{\text{eff}}(\text{AX})$ measured at room temperature and at about 80 K, the

dynamic component, B_d , the Debye temperature, θ_D , and the static component, B_s , for each constituent atom, as well as for bulk crystals, were determined. The results are summarized in Table I, where the B values of the N atom and of the bulk crystal for BN were determined from only two pairs of diffraction lines, which naturally means less accuracy in its B values.

4. Discussion

Fig. 2 shows the Debye temperatures of the bulk crystals and of their metal components plotted against the published values [6]. Although we have only four points for θ_D (bulk) for the compounds because of the lack of published data, the θ_D (X-ray) of the bulk crystals, except KBr, result in smaller values than

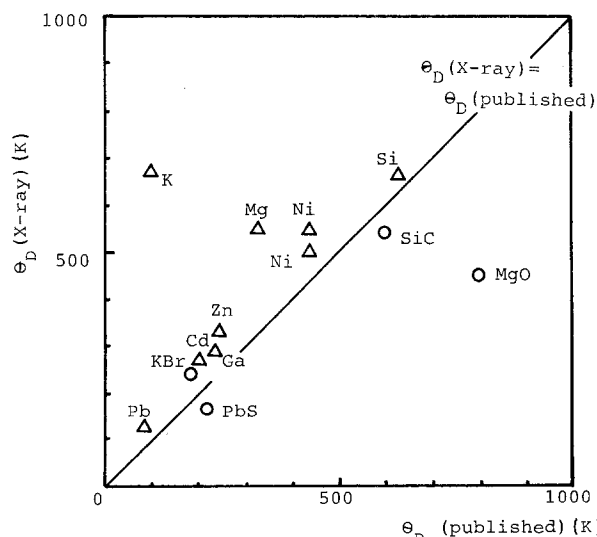


Figure 2 The observed Debye temperature, θ_D (X-ray), plotted against the Debye temperature determined from specific heat and elastic constants, θ_D (published). (○) Bulk crystal, (△) metal component in the compound.

those published which were determined mostly from specific heat. This might be due to the presence of the static component, B_s , in the crystals, as discussed previously [1, 2] for monoatomic crystals. The metal atoms in compounds yield much higher θ_D values than in pure metals; in other words, the thermal vibration of metal atoms is more constrained in compounds than in metals. This is believed to be reasonable because of the presence of static component, B_s , and the observed thermal vibration of metal atoms in the restricted space of oppositely charged atoms.

The samples of NiO were prepared in purified argon gas flow and in air, the former being reasonably supposed to have lower degree of non-stoichiometry than the latter. These two samples show quite different values of B_{eff} ; the latter contains a larger amount of defects and gives B_{eff} values close to twice that of the former, the difference being mainly a result of the B_s component. This suggests a remarkable effect of structural defects on the X-ray Debye–Waller parameters.

The samples of SiC, which were prepared with differing degrees of reaction between solid carbon and fused silicon, give higher values of B_{eff} than for pure SiC, which is not only due to the high B_s value, but also due to the high B_d value (i.e. a low Debye temperature).

The dynamic components (B_d) for constituent atoms, $B_d(A)$ and $B_d(X)$, are plotted against those for bulk crystal $B_d(AX)$ in Fig. 3, where the open symbols represent the values for the heavy atoms and the closed symbols those for the light atoms (in KBr and ZnTe, Br and Te are the heavy atoms, respectively). It is worth noting that with most of the crystals the dynamic component for the heavy atom is closer on average to the 45° line (which signifies the locus of equal dynamic components for the bulk crystal and constituent atoms) than that for the light atom. In other words, the dynamic component of the bulk

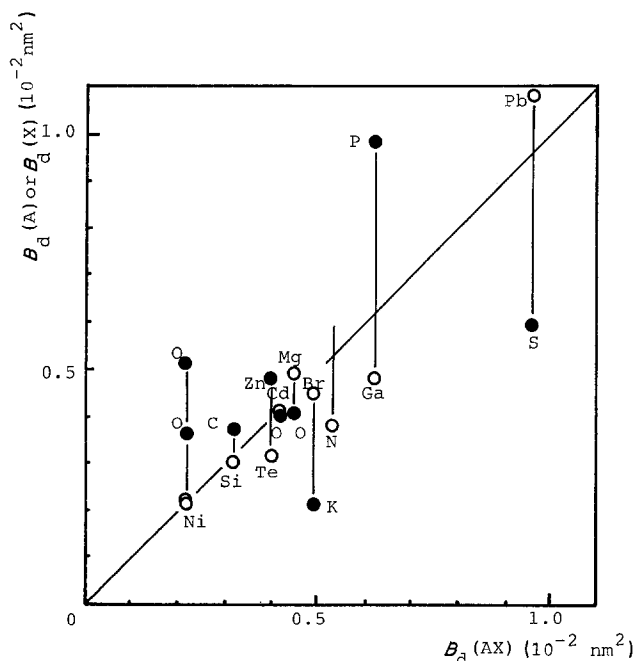


Figure 3 Relations between the dynamic component for constituent atoms $B_d(A)$ and $B_d(X)$ and that for the bulk $B_d(AX)$. The 45° line signifies the locus of $B_d(AX) = B_d(A)$ or $B_d(X)$. (○) Heavy atom, (●) light atom.

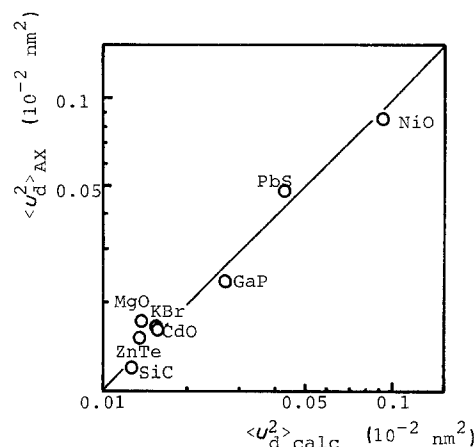


Figure 4 Coincidence of mean square displacement measured on the bulk crystals, $\langle u^2 \rangle_{\text{AX}}$, to that calculated from atomic components by Equation 9, $\langle u^2 \rangle_{\text{calc}}$.

crystal is mostly determined by the heavy atom. With BN, the dynamic component for the light atom, B, could not be determined (see Table I). That is why nitrogen does not have a partner in Fig. 3.

Because of the dominant effect of the heavy atom on $B_d(AX)$, the mean square displacement $\langle u^2 \rangle_{\text{calc}}$ for the bulk crystal was approximated by the atomic mass averaged square displacements of each atom, $\langle u^2 \rangle_A$ and $\langle u^2 \rangle_X$, as follows:

$$\langle u^2 \rangle_{\text{calc}} = [m_A / (m_A + m_X)] \langle u^2 \rangle_A + [m_X / (m_A + m_X)] \langle u^2 \rangle_X \quad (9)$$

and plotted in Fig. 4 against the observed $\langle u^2 \rangle_{\text{AX}}$ of the bulk crystals, which were derived from $B_d(AX)$. The excellent coincidence between the two $\langle u^2 \rangle$ values suggests that the average thermal vibration over the diatomic crystal is well represented by the mass-weighted proportion of thermal vibrations by the constituent atoms (Equation 9), where m_A and m_X are the masses of atoms A and X, respectively.

From Table I and Fig. 3, the oxide ions in MgO, NiO and CdO are seen to have almost the same values of dynamic component, B_d , which is reasonable because they are constructed of the same close-packed face-centred cubic lattice of oxide ions.

References

1. M. INAGAKI, Y. SASAKI and M. SAKAI, *J. Mater. Sci.* **18** (1983) 1803.
2. M. INAGAKI, Y. SASAKI and T. HIGASHI, M. TOYODA and M. SAKAI, *ibid.* **21** (1986) 566.
3. B. E. WARREN, "X-Ray Diffraction" (Addison-Wesley, Massachusetts, 1969) p. 61.
4. J. S. KASPER and K. LONSDALE (eds), "International Tables for X-ray Crystallography", Vol. 2 (Kynoch, Birmingham, 1972) p. 264.
5. M. INAGAKI, Y. SASAKI, S. NARIMATSU and M. SAKAI, *Adv. X-ray Anal.* **12** (1980) 13.
6. G. BUSCH and H. SCHADE, "Lectures on Solid State Physics" (Pergamon, Oxford, 1976) p. 63.

Received 5 June 1986
and accepted 4 March 1987